RESEARCH ARTICLE OPEN ACCESS

Association of Plaque Morphology With Stroke Mechanism in Patients With Symptomatic Posterior Circulation ICAD

Xiaoyan Song, MD,* Shuang Li, MD,* Heng Du, MD, Qimin Hu, MD, Li Zhou, MD, PhD, Jinglong Zhao, MD, PhD, Yue Gu, MD, Yiming Hu, MD, Haiyan Lu, MD, PhD, Guodong Wang, MD, Xiangyan Chen, MD, PhD,† and Qiaoshu Wang, MD, PhD†

Correspondence
Dr. Wang
qwang624@139.com

Neurology® 2022;99:e2708-e2717. doi:10.1212/WNL.0000000000201299

Abstract

Background and Objectives

Although the main mechanisms of stroke in patients with intracranial atherosclerotic disease (ICAD)—perforating artery occlusion (PAO) and artery-to-artery embolism (AAE)—have been identified and described, relatively little is known about the morphology of the symptomatic plaques and how they differ between these 2 mechanisms.

Methods

We prospectively recruited patients with acute ischemic stroke in the posterior circulation that was attributable to ICAD. Fifty-one eligible patients were enrolled and underwent magnetic resonance imaging before being assigned to the PAO or AAE group according to probable stroke mechanism. Plaque morphological properties including plaque length, lumen area, outer wall area, plaque burden, plaque surface irregularity, vessel wall remodeling, and plaque enhancement were assessed using high-resolution MRI. Plaque morphological parameters of both PAO and AAE groups were compared using nonparametric tests. A binary logistic regression model was used to identify independent predictors while a receiver operating characteristic curve tested the sensitivity and specificity of the model.

Results

Among patients who met the imaging eligibility criteria, 38 (74.5%) had PAO and 13 (25.5%) had AAE. Plaque length was shorter (6.39 interquartile range [IQR, 5.18–7.7]1 mm vs 10.90 [IQR, 8.18–11.85] mm, $p < 0.01$) in patients with PAO. Plaque burden was lower in PAO group (78.00 [IQR, 71.94–86.35] % vs 86.37 [IQR, 82.24–93.04] %, $p = 0.04$). The proportion of patients with plaque surface irregularity was higher in patients with AAE than in patients with PAO (19/38, 50.00% vs 12/13, 92.30%, $p = 0.008$). Plaque length was significantly associated with the PAO mechanism (adjusted OR 0.57, 95% CI, 0.41–0.79).

Discussion

Intracranial atherosclerotic plaque morphology differs between patients with PAO and those with AAE. Plaque with shorter length, lower plaque burden, and regular surface is more likely to cause PAO.

RELATED ARTICLE

Editorial
Intracranial Plaque Imaging
Page 1079

*These authors contributed equally to this work as first authors.

†These authors contributed equally to this work as senior authors.

From the Departments of Neurology (X.S., Q.H., Y.G., Y.H., H.L., G.W., Q.W.)Radiology (J.Z.), Shanghai General Hospital, Shanghai Jiao Tong University School of Medicine; Departments of Medicine and Therapeutics (S.L.), The Chinese University of Hong Kong, Prince of Wales Hospital, Shatin; Department of Health Technology and Informatics (H.D., X.C.), The Hong Kong Polytechnic University, Hung Hom, Kowloon; Department of Psychology (L.Z.), Faculty of Medicine, The Chinese University of Hong Kong, Shatin, China.

Go to Neurology.org/N for full disclosures. Funding information and disclosures deemed relevant by the authors, if any, are provided at the end of the article.

The Article Processing Charge was funded by the authors.

Glossary

AAE = artery-to-artery *embolism*; **ADC** = apparent diffusion coefficient; **BA** = basilar artery; **DWI** = diffusion-weighted imaging; **FOV** = field of view; **HRMRI** = high-resolution MRI; **ICC** = intraclass correlation coefficient; **ICAD** = intracranial atherosclerotic disease; **ICVA** = intracranial segment of VA; **IQR** = interquartile range; **MRA** = MR angiography; **OWA** = outer wall area; **PAO** = perforating artery occlusion; **PCA** = posterior cerebral artery; **ROC** = receiver operating characteristic; **TR/TE** = repetition time/echo time; **VA** = vertebral artery.

Intracranial atherosclerotic disease (ICAD) is one of the leading causes of ischemic stroke worldwide, particularly in East Asian, Hispanic, and African American populations with high rates of morbidity and mortality.[1-5] In contrast to symptomatic carotid artery stenosis where artery-to-artery embolism (AAE) has long been regarded as the main mechanism for stroke in the setting of moderate-to-severe internal carotid artery plaque,[6,7] less is known about perforating artery occlusion (PAO) which may play a more important role in patients with ICAD.[8,9] In the posterior circulation, ICAD is frequently present in the distal vertebral artery (VA) and the basilar artery (BA). In clinical practice, diffusion-weighted imaging (DWI) is used to explore the association between ischemic lesions responsible for stroke and intracranial atheromatous disease.[10] It has been widely accepted that intracranial occlusive diseases often cause pontine or medullary infarcts in the supply zone of one of the paramedian branches of the BA or distal VA. Otherwise, artery-to-artery emboli from ICAD could potentially lead to cortical infarcts in the cerebellum or temporo-occipital lobe, or to multiple infarcts, including the "top of the basilar" syndrome.[11-13] Despite a variety of possibilities, the specific properties that determine whether intracranial atherosclerotic plaques will be occlusive or embolic remains unclear.

With the development of neuroimaging techniques, some subcortical lacunar–like infarcts have been identified and found to be caused by large-artery atherosclerosis rather than by small vessel diseases such as lipohyalinosis.[14] However, recent research has proposed that using traditional imaging techniques such as MR angiography (MRA), CT angiography, and transcranial Doppler may not be sensitive enough to accurately detect plaque morphology or the true mechanism of stroke (e.g., a number of patients with perforating artery infarction exhibited no apparent narrowing)—especially in the posterior circulation with abundant branches, where PAO is responsible for 35.9% of all infarct patterns.[8,15,16]

Therefore, recent advances in neuroimaging such as high-resolution MRI (HRMRI) may provide new insights into the interaction between plaque morphology and stroke mechanisms.[16,17] In this study, we identified and measured intracranial posterior circulation plaque morphology using HRMRI. We assessed morphological properties of plaques such as length, surface irregularity, and plaque burden and correlated the plaque morphological properties with the ICAD mechanisms of PAO and AAE using state-of-the-art imaging techniques in MRI.

Methods

Study Population

For this multicenter, observational study, we prospectively recruited patients with acute stroke with ICAD in the posterior circulation within 7 days of symptom onset. All patients underwent head HRMRI, MRA, and DWI. The etiologic origins of each stroke and its relevance to ICAD were determined by clinical neurologists using the ASCO (Atherosclerosis, Small vessel disease, Cardiac source, Other cause) stroke subtype classification.[18] Patients were considered for inclusion if within the preceding week (1) they had an ischemic stroke in the distribution of posterior circulation, (2) a hyperintense signal was seen on DWI while an associated decrease in signal was seen on the apparent diffusion coefficient (ADC) map, and (3) symptomatic eccentric atherosclerotic plaques were identified within the intracranial posterior circulation, including the intracranial segment of VA (ICVA), the BA, and P1 segment of the posterior cerebral artery (PCA) on HRMRI. We then classified the mechanisms of ICAD into 2 groups—PAO and large-artery occlusive disease AAE based on previously published criteria (Figures 1and 2).[8,9] Patients with any of the following features were excluded from the analysis: (1) probable nonatherosclerotic vasculopathy, such as Moyamoya disease, vasculitis, or dissection; (2) evidence of cardioembolism; (3) coexistent > 50% extracranial VA stenosis or luminal irregularity.

Standard Protocol Approvals, Registrations, and Patient Consents

The Shanghai General Hospital Clinical Research Ethics Committee approved the study (Reference No. 2016KY164-3), and each participant provided written informed consent.

MRI Protocol

MRI was performed with a 3.0 Tesla MR Achieva scanner (Philips Healthcare, Best, Netherlands) and an eight-channel phased array coil within 7 days from the index stroke. All patients initially underwent conventional brain MRI, which included T1-weighted and T2-weighted imaging, T2 fluid-attenuated inversion recovery, DWI, ADC, and 3-dimensional (3D) time-of-flight (TOF) MRA. DWI was performed with the following parameters: a slice thickness of 5 mm (no gap between slices) with a matrix size of 128 × 128 mm, 24–30 axial slices, a field of view (FOV) of 240 mm, a standard spin echo echo-planar imaging sequence with a repetition time/echo time (TR/TE) =4,528/103 m. The 3D TOF MRA images were obtained using the following parameters: TR/TE = 23.0/3.5 ms,

flip angle = 25°, FOV = 160 × 160 mm, acquired resolution 0.55 × 0.55 × 1.1 mm, and reconstructed resolution 0.55 × 0.55 × 0.55 mm.

HRMRI was obtained on the stenotic lesions identified by TOF-MRA. The 3D high-resolution black-blood (BBMRI) sequence was performed using a volumetric isotropic turbo spin echo acquisition (VISTA; Philips Healthcare, Best, Netherlands) in a coronal plaque (40-mm thick slab) optimized for flow suppression and intracranial vessel wall delineation. The BBMRI sequence were acquired using the following parameters: FOV = 200 × 167 × 45 mm, acquired resolution 0.6 × 0.6 × 1.0 mm, reconstructed resolution = 0.5 × 0.5 × 0.5 mm, TR/TE = 1500 ms/36 ms; turbo spin echo factor 56 echoes, echo spacing 4.0ms, sense factor 1.5 (right-left direction), scan time of 6.51 minutes. Before the acquisition of the contrast-enhanced T1 VISTA sequence, a gadolinium-containing contrast agent (Dotarem, Gadoteric acid 0.5 mmol/mL; Guerbet, Roissy CdG Cedex, France) was introduced intravenously (0.1 mmol per kilogram of body weight) and BBMRI was repeated 5 minutes after contrast material administration.

MRI Analysis

The lesion sites for evaluation of symptomatic atheromatous plaques were determined by 1 neurologist (Q.W.) and 1 neuroradiologist (J.Z.) with more than 25 years' experience in interpreting and researching neurovascular images. In patients with more than 1 spatially separated, qualifying ICAD lesion, the plaque with the highest degree of luminal stenosis was measured. If any disagreements arose between the 2 senior clinicians, a third senior neuroradiologist's decision was obtained. In this study, an acute infarct was defined as a hyperintense signal on DWI with an associated hypointense signal on the ADC map. Based on their size and number, infarcts were categorized as (1) small lesions (diameter <20 mm) or large lesions (diameter ≥20 mm); (2) single infarct (only 1 contiguous acute lesion identified on DWI) or multiple infarcts. Patients were assigned to 1 of 2 group according to probable stroke mechanism: PAO or AAE (Figures 1 and 2). The PAO group included patients with acute infarct(s) within the territory of the perforating branches where atherosclerotic plaque had occluded the orifice (Figure 3). The AAE group included patients with moderate-to-severe stenosis (50%–99% luminal narrowing) in the intracranial artery that correlated with infarcts distributed in multiple distal territories such as the medulla, cerebellum, occipital lobe, and temporal lobe (where either ipsilateral or bilateral areas were involved) (Figure 4). The degree of luminal stenosis was measured on TOF MRA according to the Warfarin Aspirin Symptomatic Intracranial Disease study.[19]

Image analysis was performed using Osirix MD (Ver.11.0.3, Pixmeo) software to reconstruct the cross-sections of vessel walls. If a markedly eccentric wall thickening was evident on the HRMR images, it was defined as atherosclerotic plaque.[17] VesselMass (Leiden University Medical Center, Netherlands)

Figure 1 Flowchart of Participant Recruitment and Criteria for Imaging Analysis

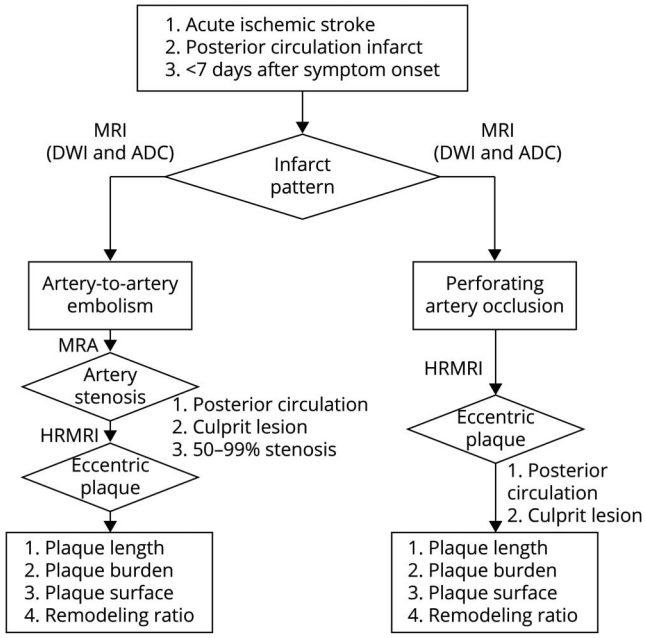

Brain magnetic resonance imaging (MRI) including diffusion-weighted imaging (DWI), apparent diffusion coefficient (ADC) map, magnetic resonance angiography (MRA), and high-resolution MRI (HRMRI) were used to interpret the stroke mechanisms. Based on the infarct patterns on DWI and ADC map, participants were screened and divided into 2 groups: (1) artery-to-artery embolism (AAE) group and (2) perforating artery occlusion (PAO) group.

software was used to measure the reconstructed images. Lumen and outer wall contours were drawn on each pertinent slice in the sequence which automatically generated statistics that included wall area (OWA), lumen area (LA), and wall area (WA= OWA – LA) (Figures 3 and 4). Plaque length was defined as plaque slices × slice thickness. Plaque burden was calculated as WA/OWA × 100%. The OWAs at the reference sites (the distal and proximal sites) were also measured. The reference OWA ($OWA_{reference}$) was defined as the mean of distal and proximal OWAs. The arterial remodeling ratio (RR) was calculated as $OWA/OWA_{reference}$. RR ≥ 1.05 was considered as positive remodeling, RR ≤ 0.95 negative remodeling, and 0.95 < RR < 1.05 as intermediate remodeling.[20,21] Plaque surface was classified as irregular if there was a discontinuity of the plaque surface margin or a disruption of the plaque inner wall (Figures 2 and 4).[22]

Statistical Analysis

Quantitative data were expressed as median (interquartile range [IQR]) and compared using a between-groups Mann-Whitney test. Categorical variables were summarized as count (percentage) and analyzed using the χ^2 test or the Fisher exact test. Furthermore, in a multiple binary logistic regression model, we tested for an independent relationship between plaque features and the stroke mechanisms of PAO and AAE after adjusting for factors with $p < 0.10$ in univariable logistic regression analyses. Variables with p values less than 0.1 from

Figure 2 Mechanisms of Artery-to-Artery Embolism (AAE) and Perforating Artery Occlusion (PAO)

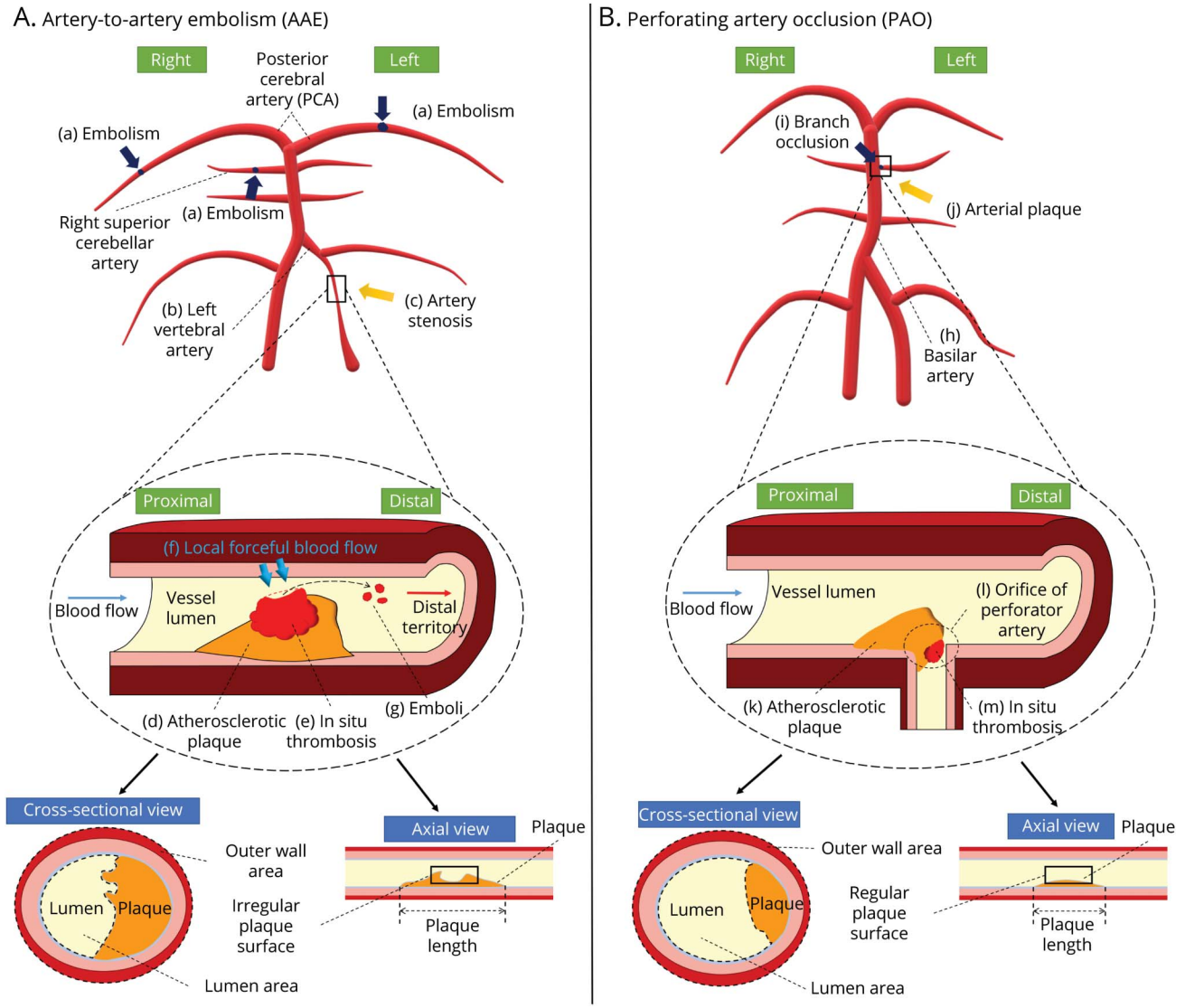

(1) The left diagram shows that AAE leads to the infarct pattern of multiple embolisms (A) in separate distal territories (cortical and subcortical) of the culprit artery. The left vertebral artery (B) with stenotic lesion (C) is the culprit artery segment. Beginning with fissuring of the fibrous cap of the atherosclerotic plaque (D), in situ thrombosis (E) can be formed rapidly. During this process, local forceful blood flow (F) may break up a part of the thrombus and carry the emboli (G) to distal arteries. (2) The right diagram shows PAO mostly caused by eccentric plaque associated with small single subcortical infarct. A branch of the basilar artery (H) with relatively normal vessel lumen is occluded (I) due to atherosclerotic plaque (J). PAO mainly results from the protrusion of the atherosclerotic plaque (K) of the parent artery into the orifice of the perforator artery (L), in which secondary thrombosis (M) can be formed.

univariate analyses were considered candidate predictors, and Forward: LR was used to select variables including plaque length, plaque burden, and stenosis degree. The receiver operating characteristic (ROC) curve was calculated based on the logistic regression model. The highest value of the Youden index was used to determine the cut-off point for the model-predicted probability that reported the sensitivity and specificity of the model. A p value of less than 0.05 indicated statistical significance. Inter-reader reliability was assessed by using intraclass correlation coefficients (ICCs) with a two-way random effects model for continuous variables. Reliabilities less than 0.4 were considered as poor, 0.4–0.75 as fair, and above 0.75 as excellent. All statistical analyzes were performed using SPSS 23.0 (IBM SPSS Inc, Chicago, IL).

Results

Participant Characteristics

From March 2017 to May 2019, we recruited 51 patients with acute stroke with symptomatic ICAD in the posterior circulation; 38 with PAO, and 13 with AAE (see Table 1 for patient demographic data). Traditional stroke risk factors were similar between the 2 groups. In the PAO group, most of the infarcts were detected in the pons (36/46, 78.3%), yet in AAE group, the 34 infarcts seen in the group's images were located in numerous different regions within the posterior circulation, with larger concentrations in the cerebellum (9/34, 26.5%) and occipital lobe (6/34, 17.6%).

Figure 3 High-Resolution MRI (HRMRI) of Basilar Artery Plaque With Perforating Artery Infarct

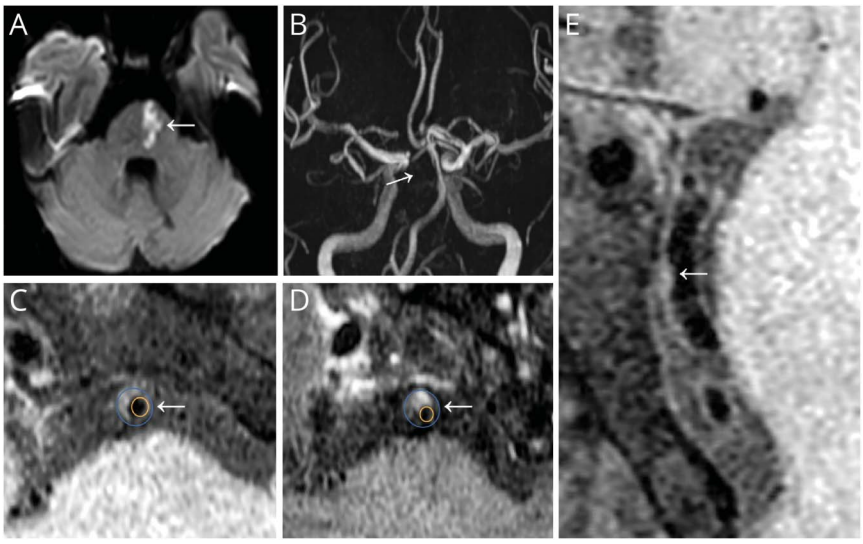

A transverse MRI showed an acute left pontine infarct (arrow) on DWI (A) with mild stenosis (arrow) in basilar artery on MRA (B). HRMRI showed an eccentric wall thickening (arrow) in corresponding site with contrast enhancement in cross-section imaging (C and D, the plaque enclosed by blue contour represents the outer wall area and yellow contour represents lumen area). Arrow showed regular plaque surface in long axis of HRMRI (E). Abbreviation: DWI = diffusion-weighted imaging.

Plaque Morphology and Infarct Patterns

Plaque morphological characteristics are summarized in Table 2. In the PAO group, we found that symptomatic plaques were commonly located in the BA (30/38, 78.9%), while in the AAE group, most of the lesions were found in the intracranial VA (5/13, 38.5%) and the BA (6/13, 46.2%). Compared with the PAO group, the degree of stenosis was significantly higher (55 [48–66] % vs 69 [65–77]%, $p = 0.001$) in the AAE group, and the degree of plaque burden in the PAO group was significantly lower than that in the AAE group (78.00 [71.94–86.35]% vs 96.37 [82.24–93.04]%, $p = 0.04$). Of the 51 symptomatic plaques, 33 (64.7%) showed contrast enhancement, and no significant differences were identified between the PAO and AAE groups in this area. Plaque length in patients with PAO was significantly shorter than that seen in patients with AAE (6.39 [5.18–7.71] mm vs 10.90 [8.18–11.85] mm, $p < 0.01$). Among the 51 ICAD plaques detected in the posterior circulation, positive remodeling was identified in 31 (60.8%) plaques and negative remodeling was seen in 18 (35.3%). There were no significant differences between the 2 groups in the positive to negative ratio of remodeling in plaque areas (Table 2).

Figure 4 High-Resolution MRI (HRMRI) of Basilar Artery Plaque With Artery-to-Artery Emboli

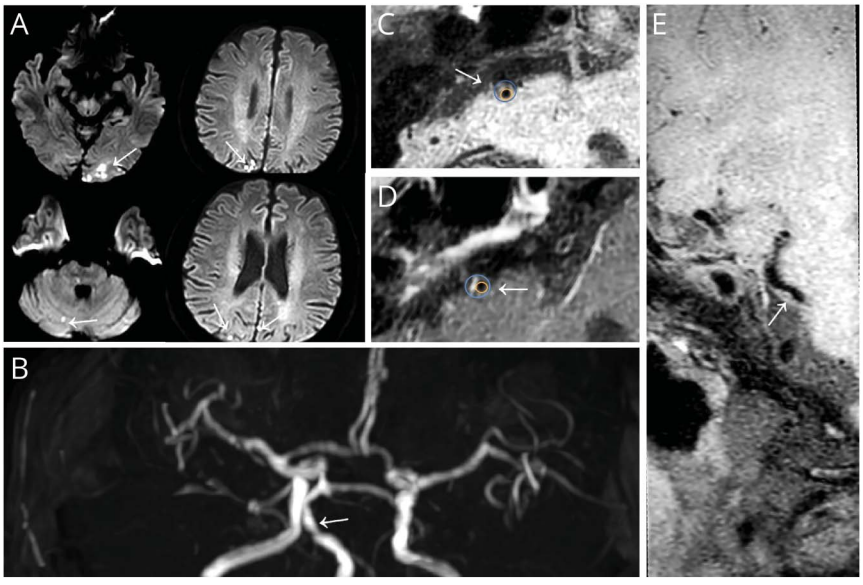

A patient with multiple acute infarcts in cerebellum and bilateral occipital lobe (arrow) on DWI (A) with severe stenosis (arrow) in basilar artery on MRA (B). HRMRI showed an eccentric wall thickening (arrow) in corresponding site with contrast enhancement in cross-section imaging (C), the plaque enclosed by blue (outer wall area) and yellow (lumen area) contour. Arrow showed irregular plaque surface in long axis of HRMRI (D). Abbreviation: DWI = diffusion-weighted imaging.

Table 1 Patient Demographic Data by PAO and AAE Group

Population	PAO (n = 38)	AAE (n = 13)	*p* Value
Age (y)	62 (59–69)	64 (56–74)	0.59
Male	28 (73.7%)	9 (69.2%)	0.734
Smoking history	11 (28.9%)	8 (61.5%)	0.05
Hypertension	28 (73.7%)	9 (69.2%)	0.734
Diabetes mellitus	23 (60.5%)	4 (30.8%)	0.064
LDL (mmol/L)	2.74 ± 1.05	2.43 ± 0.83	0.41
Total cholesterol (mmol/L)	4.50 ± 1.51	4.20 ± 1.02	0.56
Infarct sites	46	34	
Medulla	9 (19.6%)	2 (5.9%)	
Pons	36 (78.3%)	6 (17.6%)	
Midbrain	0	4 (11.8%)	
Cerebellum	0	9 (26.5%)	
Occipital lobe	0	6 (17.6%)	
Temporal lobe	0	4 (11.8%)	
Thalamus	1 (2.2%)	2 (5.9%)	
Callosum	0	1 (2.9%)	

AAE = artery-to-artery embolism; LDL = low density lipoprotein; n = number of subjects; PAO = perforating artery occlusion.

Plaque surface irregularity was identified in 31 (60.8%) patients and was more likely to be found in the AAE group (19/38, 50.0% vs 12/13, 92.3%, $p = 0.008$). Irregular plaque surface was more common in patients with multiple infarcts (19/27, 70.4% vs 12/24, 50.0%, $p = 0.161$) (Table 3). Among the 51 patients with ICAD in the posterior circulation, we found small-size infarcts in 42 (82.4%) patients and a single infarction in 24 (47.1%). The proportion of small-size infarctions (34/38, 89.5% vs 8/13, 61.5%, $p = 0.003$) and single infarction (23/38, 60.5% vs 1/13, 7.7%, $p = 0.001$) were significantly higher in PAO group (Table 2).

A binary logistical regression was used to identify independent predictors of plaques related to PAO. We found that plaque length was independently associated with the PAO mechanism (adjusted OR 0.573, 95% CI, 0.41–0.79, $p = 0.001$). The area under the ROC curve was 0.86 (95% CI, 0.74–0.99), which provided a sensitivity of 76.3% and a specificity of 92.3% in predicting PAO. No evidence of multicollinearity was found in our regression analyses.

Measurement Reliability

The inter-reader reliability for LA, OWA, RR, and plaque length with ICC (95% CI) were 0.90 (0.80–0.95), 0.84 (0.70–0.92), 0.893 (0.79–0.94), and 0.76 (0.54–0.87), respectively.

Discussion

In this hospital-based multicenter study, we reported the morphological features of symptomatic plaques in the intracranial posterior circulation and their possible correlation with stroke mechanisms. Our study provided evidence that plaque features differ between patients with PAO and patients with AAE. Compared with plaques in the AAE group, plaques in the PAO group had a shorter length, a lower plaque burden, and a relatively regular surface. Plaque length was independently associated with PAO.

For several decades, lumen stenosis has been the primary object studied in many investigations focused on symptomatic ischemic events.[22,23] However, with the recent advances in neuroimaging technology, some factors have been both verified and shown to be at least equally (if not more) effective in the evaluation of ischemic stroke than the older methods.[24,25] The vessel wall imaging using HRMRI is sensitive enough to enable the delineation of vessel wall changes caused by intracranial atherosclerosis or other etiology, such as vasculitis or dissection. For stroke patients with intracranial atherosclerosis, adding a group of measurable morphological features (e.g., plaque burden, plaque length, lesion eccentricity, and remodeling ratio) to the time-tested lumen stenosis identification may improve clinician's ability to detect the presence of ICAD in the posterior circulation, categorize symptomatic plaque, and quantitatively assess the degree of stroke risk and/or recovery potential.[26-29] Apart from predicting the occurrence of ischemic events, the new imaging features could also be used to infer the underlying mechanism, together with other information such as location, size, or number of brain infarcts. PAO could be the result of atherosclerotic plaques without causing lumen narrowing >50% identified on MRA. In a HRMRI study among patients with paramedian pontine infarction, HRMRI detected a plaque in 61.5% of patients, whereas only 35% had BA lumen stenosis on conventional TOF MRA.[30] Therefore, ASCO (Atherosclerosis, Small vessel disease, Cardiac source, Other cause) stroke subtype classification proposed HRMRI as a useful method to identify stroke phenotype characterization and mechanism.[18]

In the PAO group, most of these infarcts were found in the pons close to the responsible vessels. Furthermore, isolated lesions are commonly detected in this type of infarct. By contrast, in the AAE group, multiple infarcts were common and often found in distal regions of the posterior circulation, especially the cerebellum and the occipital lobe. This result is consistent with a previous study that found the cerebellum is often involved in atherosclerotic strokes when there are multiple infarcts.[31] We also found that in both groups, half of the responsible vessels were in the BA. Studies indicated that in strokes caused by intracranial atherosclerosis, symptomatic plaques were most often detected in the middle BA.[32,33] Of note, the authors of a study also found that plaques located at this site presented at a higher rate in recurrent strokes or death.[32]

Table 2 Comparison of Plaque Morphology Between PAO Group and AAE Group

	PAO (n = 38)	AAE (n = 13)	*p* Value
Location of symptomatic plaques			
Intracranial vertebral artery	7 (18.4%)	5 (38.5%)	
Basilar artery	30 (78.9%)	6 (46.2%)	
Posterior cerebral artery	1 (2.6%)	2 (15.4%)	
LA (mm^2)	5 (3–10)	4 (2–19)	0.115
OWA (mm^2)	25 (19–45)	20 (17–70)	0.252
Plaque burden (%)	78.00 (71.94–86.35)	86.37 (82.24–93.04)	0.04[a]
Stenosis degree (%)	55 (48–66)	69 (65–77)	0.001[a]
Plaque enhancement	22 (57.89%)	11 (84.61%)	0.103
Plaque length (mm)	6.39 (5.18–7.71)	10.90 (8.18–11.85)	<0.01[a]
Remodeling ratio	1.14 (0.88–1.40)	1.12 (0.87–1.99)	0.489
Vessel wall remodeling			0.626
Positive	23 (60.5%)	8 (61.5%)	
Intermediate	1 (2.6%)	1 (7.7%)	
Negative	14 (36.8%)	5 (30.8%)	
Small-size infarct	34 (89.5%)	8 (61.5%)	0.036[b]
Single infarct	23 (60.5%)	1 (7.7%)	<0.01[b]

PAO, perforating artery occlusion; AAE, artery-to-artery embolism; LA, lumen area; OWA, outer wall area.
[a] Mann-Whitney *U* test.
[b] Fisher exact test.

Regarding plaque burden, a larger plaque volume may increase stroke risk due to more severe lumen narrowing or PAO. Our study indicated that a higher atherosclerosis burden was more likely to cause AAE, which concurs with studies of symptomatic carotid artery stenosis.[6,7] A study of Hong Kong Chinese who had acute strokes with moderate-to-severe middle cerebral artery stenosis (>50-99%) showed that (1) multiple cerebral emboli is an important mechanism of cerebral infarcts and (2) microembolic signals were detected in 9 (60%) patients with multiple infarcts and in 1 (6.6%) patient with a single infarct.[34] In previous studies of anterior circulation, researchers suggested that in MCA strokes, plaque burden tended to be lower in deep perforator infarctions in asymptomatic atherosclerotic plaque.[28,35] Similarly, we also observed that the plaque burden appeared significantly lower in cases of PAO of posterior circulation.

As for plaque length, we found that it was significantly shorter in patients with PAO compared with those with AAE. A logistic regression model also showed that plaque length may serve as an independent predictor of PAO or AAE as a mechanism for stroke. Knowledge from an extracranial carotid atherosclerosis (>65% stenosis) study indicated that carotid plaque length was a significant variable (in addition to

Table 3 Plaque Surface Irregularity

	Multiple infarcts		Single infarct		
	Normal	Irregularity	Normal	Irregularity	Total
PAO	8	7	11	12	19/38 (50.0%)[a]
AAE	0	12	1	0	12/13 (92.3%)[a]
Total	8	19/27 (70.4%)[b]	12	12/24 (50.0%)[b]	31/51 (60.8%)

PAO = perforating artery occlusion; AAE = artery-to-artery embolism.
[a] PAO vs AAE (p = 0.008, Fisher exact test).
[b] Multiple vs single (p = 0.161, Pearson chi-square).

degree of stenosis), in predicting compromise of ipsilateral carotid blood flow in patients undergoing carotid revascularization.[36] Similar findings were obtained in another study in patients with symptomatic carotid artery atherosclerosis whose carotid plaque length was independently associated with microembolic signals.[37] This mechanism may help explain why increasing plaque length is related to AAE.

In addition, we noted significant plaque surface irregularity in the AAE group compared with the PAO group. A study defined surface irregularity as a discontinuity of the surface or disruption of the plaque inner wall.[22] Another study reported that such surface irregularity was strongly related to symptomatic stroke and multiple infarcts.[20,38] Multiple infarcts, usually refer to artery-to-artery emboli and present the most common pattern in both anterior and posterior circulation.[15] As we speculate, atherosclerosis with surface irregularity may indicate the presence of plaque ulceration. Several studies have reported that plaque ulceration was the main source of microemboli and had an association with recent ischemic symptoms.[39,40]

The problem of vessel wall remodeling has been investigated in numerous studies. Positive remodeling is a term describing the compensated enlargement of a vessel wall in response to changing hemodynamics or other factors.[21] Generally speaking, enlarged arteries provide greater volume/blood supply in the presence of atherosclerotic plaques. However, in many cases, that volume can actually be considered as a red flag for unstable plaque which is not only inclined to rupture but also can occlude arteries downstream and thus lead to more damaging ischemic events.[21,38,41] In our study, we found that positive remodeling happened with equal frequency in both the PAO and AAE groups. Several studies indicated that symptomatic plaques had higher remodeling ratios and frequency of positive remodeling.[26,42,43] Beyond that, positive remodeling is generally related to other aspects of ischemic stroke. The authors of a study proposed that positive remodeling is related to serious clinical symptoms.[44] They measured the NIHSS scores of patients with stroke and found that scores were higher in patients with positive remodeling than in those with negative remodeling. Through the use of transcranial color Doppler, the authors of a study found that greater numbers of microemboli were detected in patients with positive remodeling.[45] In our research, while the prevalence of positive remodeling proved to be similar between the PAO and AAE groups, the remodeling ratio was higher in the AAE group but not statistically significant.

Of note, our study has indicated that plaques with longer length and irregular surfaces present a greater risk for artery-to-artery emboli. With this in mind, we hypothesize that, the greater the plaque burden, the more unstable the inner substance and the more likely it would be to damage the plaque surface and form thrombin that could embolize downstream. Considering that intracranial plaques with long length, greater plaque burden, and irregular surface may be responsive to dual antiplatelet therapy, and antiplatelet therapy has been shown to reduce microemboli in carotid stenosis,[46,47] we believe our findings have therapeutic implications for early detection with HRMRI and treatment with dual antiplatelet therapies.

Our study has several limitations. First, previous studies found that atherosclerosis affected both the extracranial VA (ECVA) and the intracranial posterior circulation equally.[48-50] The main mechanism of symptomatic ECVA is AAE. In our series, patients with ECVA stenosis were not recruited, which leads to fewer patients in the AAE group. Second, when evaluating the vessel wall with HRMRI, the interpreters were not blind for the ICAD stroke subtype, which may have influenced their views of the data analysis. Third, in vivo evaluation of intracranial vessel wall lesions and plaque properties is inherently challenged by the lack of histologic correlations. Fourth, in our study, all intracranial posterior circulation arteries, including ICVA, BA, and PCA, were analyzed together to explore the mechanism of stroke. In different cohorts, the proportion of vessels may be variable, which may, in turn, have some degree of influence on our results. Owing to the limited sample size, no vessel-specific studies on BA or ICVA were performed. Finally, plaque morphology data on HRMRI such as intraplaque hemorrhage, calcification, and plaque volume were not included as outcome variables here and thus will be targets for analysis in future studies.

Overall, our findings showed that HRMRI is helpful for exploring symptomatic atherosclerotic plaque morphology in the posterior circulation with PAO or AAE. Plaque with short length and a regular surface was associated with PAO, while plaque with long length, greater plaque burden, and an irregular surface was highly suggestive of an unstable lesion that might lead to AAE. Further longitudinal studies are required to evaluate the plaque morphology dynamically, which is likely to be helpful in providing individualized therapies as we gain a clearer and deeper understanding of the mechanisms of ischemic stroke caused by symptomatic ICAD.

Acknowledgment

The authors appreciate the study participants and all researchers who contributed to patient recruitment and data analysis.

Study Funding

This study is supported by grant from the Clinical Research Plan of SHDC (16CR2046B), grant from the National Natural Science Foundation of China (81371304), grant from Shanghai Pujiang Program (15PJD031).

Disclosure

The authors report no relevant disclosures. Go to Neurology.org/N for full disclosures.

Publication History

Received by *Neurology* April 23, 2022. Accepted in final form August 11, 2022. Submitted and externally peer reviewed. The handling editor was José Merino, MD, MPhil, FAAN.

Appendix Authors

Name	Location	Contribution
Xiaoyan Song, MD	Department of Neurology, Shanghai General Hospital, Shanghai Jiao Tong University School of Medicine, Shanghai, China.	Drafting/revision of the manuscript for content, including medical writing for content; Analysis or interpretation of data
Shuang Li, MD	Departments of Medicine and Therapeutics, The Chinese University of Hong Kong, Prince of Wales Hospital, Shatin, Hong Kong SAR, China	Drafting/revision of the manuscript for content, including medical writing for content; Analysis or interpretation of data
Heng Du, MD	Department of Health Technology and Informatics, The Hong Kong Polytechnic University, Hung Hom, Kowloon, Hong Kong SAR, China	Major role in the acquisition of data
Qimin Hu, MD	Department of Neurology, Shanghai General Hospital, Shanghai Jiao Tong University School of Medicine, Shanghai, China.	Drafting/revision of the manuscript for content, including medical writing for content
Li Zhou, MD,PhD	Department of Psychology, Faculty of Medicine, The Chinese University of Hong Kong, Shatin, Hong Kong SAR, China	Major role in the acquisition of data
Jinglong Zhao, MD,Phd	Department of Radiology, Shanghai General Hospital, Shanghai Jiao Tong University School of Medicine, Shanghai, China.	Analysis or interpretation of data
Yue Gu, MD	Department of Neurology, Shanghai General Hospital, Shanghai Jiao Tong University School of Medicine, Shanghai, China.	Major role in the acquisition of data
Yiming Hu, MD	Department of Neurology, Shanghai General Hospital, Shanghai Jiao Tong University School of Medicine, Shanghai, China.	Major role in the acquisition of data
Haiyan Lu, MD,PhD	Department of Neurology, Shanghai General Hospital, Shanghai Jiao Tong University School of Medicine, Shanghai, China.	Analysis or interpretation of data
Guodong Wang, MD	Department of Neurology, Shanghai General Hospital, Shanghai Jiao Tong University School of Medicine, Shanghai, China.	Drafting/revision of the manuscript for content, including medical writing for content
Xiangyan Chen, MD,PhD	Department of Health Technology and Informatics, The Hong Kong Polytechnic University, Hung Hom, Kowloon, Hong Kong SAR, China	Study concept or design
Qiaoshu Wang, MD,PhD	Department of Neurology, Shanghai General Hospital, Shanghai Jiao Tong University School of Medicine, Shanghai, China.	Study concept or design; Analysis or interpretation of data

References

1. Adams HP Jr., Bendixen BH, Kappelle LJ, et al. Classification of subtype of acute ischemic stroke. Definitions for use in a multicenter clinical trial. *TOAST Trial Org-stroke.* 101721993;24(1):35-41.
2. Wong LK. Global burden of intracranial atherosclerosis. *Int J Stroke.* 2006;1(3):158-159.
3. Banerjee C, Chimowitz MI. Stroke caused by atherosclerosis of the major intracranial arteries. *Circ Res.* 2017;120(3):502-513.
4. Qureshi AI, Caplan LR. Intracranial atherosclerosis. *Lancet.* 2014;383(9921):984-998.
5. Donnan GA, Fisher M, Macleod M, Davis SM. Stroke. *Lancet.* 2008;371(9624):1612-1623.
6. MRC European Carotid Surgery Trial. Interim results for symptomatic patients with severe (70-99%) or with mild (0-29%) carotid stenosis. European Carotid Surgery Trialists' Collaborative Group. *Lancet.* 1991;337:1235-1243.
7. North American Symptomatic Carotid Endarterectomy Trial Collaborators, Barnett HJM, Taylor DW, et al. Beneficial effect of carotid endarterectomy in symptomatic patients with high-grade carotid stenosis. *N Engl J Med.* 1991;325(7):445-453.
8. Kim JS, Caplan LR. Clinical stroke syndromes. *Front Neurol Neurosci.* 2016;40:72-92.
9. Wong KS, Caplan LR, Kim JS. Stroke mechanisms. *Front Neurol Neurosci.* 2016;40:58-71.
10. Lee DK, Kim JS, Kwon SU, Yoo SH, Kang DW. Lesion patterns and stroke mechanism in atherosclerotic middle cerebral artery disease: early diffusion-weighted imaging study. *Stroke.* 2005;36(12):2583-2588.
11. López-Cancio E, Matheus MG, Romano JG, et al. Infarct patterns, collaterals and likely causative mechanisms of stroke in symptomatic intracranial atherosclerosis. *Cerebrovasc Dis.* 2014;37(6):417-422.
12. Hussain Z, Hilal K, Ahmad M, Sajjad Z, Sayani R. Clinicoradiological correlation of infarct patterns on diffusion-weighted magnetic resonance imaging in stroke. *Cureus.* 2018;10(3):e2260.
13. Caplan LR. Top of the basilar syndrome. *Neurology.* 1980;30(1):72-79.
14. Adachi T, Kobayashi S, Yamaguchi S, Okada K. MRI findings of small subcortical "lacunar-like" infarction resulting from large vessel disease. *J Neurol.* 2000;247(4):280-285.
15. Lopez-Cancio E, Matheus MG, Romano JG, et al. Infarct patterns, collaterals and likely causative mechanisms of stroke in symptomatic intracranial atherosclerosis. *Cerebrovasc Dis.* 2014;37(6):417-422.
16. Klein IF, Lavallée PC, Schouman-Claeys E, Amarenco P. High-resolution MRI identifies basilar artery plaques in paramedian pontine infarct. *Neurology.* 2005;64(3):551-552.
17. Qiao Y, Zeiler SR, Mirbagheri S, et al. Intracranial plaque enhancement in patients with cerebrovascular events on high-spatial-resolution MR images. *Radiology.* 2014;271(2):534-542.
18. Amarenco P, Bogousslavsky J, Caplan LR, Donnan G, Hennerici M. New approach to stroke subtyping: the A-S-C-O (phenotypic) classification of stroke. *Cerebrovasc Dis.* 2009;27(5):502-508.
19. Weinberger J. Comparison of warfarin and aspirin for symptomatic intracranial arterial stenosis. *Curr Cardiol Rep.* 2006;8(1):7.
20. Zhao DL, Deng G, Xie B, et al. Wall characteristics and mechanisms of ischaemic stroke in patients with atherosclerotic middle cerebral artery stenosis: a high-resolution MRI study. *Neurol Res.* 2016;38(7):606-613.
21. Qiao Y, Anwar Z, Intrapiromkul J, et al. Patterns and implications of intracranial arterial remodeling in stroke patients. *Stroke.* 2016;47(2):434-440.
22. Chung GH, Kwak HS, Hwang SB, Jin GY. High resolution MR imaging in patients with symptomatic middle cerebral artery stenosis. *Eur J Radiol.* 2012;81(12):4069-4074.
23. Ryu CW, Jahng GH, Kim EJ, Choi WS, Yang DM. High resolution wall and lumen MRI of the middle cerebral arteries at 3 tesla. *Cerebrovasc Dis.* 2009;27(5):433-442.
24. Leung TW, Wang L, Zou X, et al. Plaque morphology in acute symptomatic intracranial atherosclerotic disease. *J Neurol Neurosurg Psychiatry.* 2020;92(4):370-376.
25. Leng X, Wong KS, Liebeskind DS. Evaluating intracranial atherosclerosis rather than intracranial stenosis. *Stroke.* 2014;45(2):645-651.
26. Xu WH, Li ML, Gao S, et al. In vivo high-resolution MR imaging of symptomatic and asymptomatic middle cerebral artery atherosclerotic stenosis. *Atherosclerosis.* 2010;212(2):507-511.
27. Xu WH, Li ML, Gao S, et al. Plaque distribution of stenotic middle cerebral artery and its clinical relevance. *Stroke.* 2011;42(10):2957-2959.
28. Yu YN, Li ML, Xu YY, et al. Middle cerebral artery geometric features are associated with plaque distribution and stroke. *Neurology.* 2018;91(19):e1760–e1769.
29. Dieleman N, Yang W, Abrigo JM, et al. Magnetic resonance imaging of plaque morphology, burden, and distribution in patients with symptomatic middle cerebral artery stenosis. *Stroke.* 2016;47(7):1797-1802.
30. Klein IF, Lavallee PC, Mazighi M, Schouman-Claeys E, Labreuche J, Amarenco P. Basilar artery atherosclerotic plaques in paramedian and lacunar pontine infarctions: a high-resolution MRI study. *Stroke.* 2010;41(7):1405-1409.
31. Koch S, Amir M, Rabinstein AA, Reyes-Iglesias Y, Romano JG, Forteza A. Diffusion-weighted magnetic resonance imaging in symptomatic vertebrobasilar atherosclerosis and dissection. *Arch Neurol.* 2005;62(8):1228-1231.
32. Kim YW, Hong JM, Park DG, et al. Effect of intracranial atherosclerotic disease on endovascular treatment for patients with acute vertebrobasilar occlusion. *Am J Neuroradiol.* 2016;37(11):2072-2078.
33. Samaniego EA, Shaban A, Ortega-Gutierrez S, et al. Stroke mechanisms and outcomes of isolated symptomatic basilar artery stenosis. *Stroke Vasc Neurol.* 2019;4:189-197.

34. Wong KS, Gao S, Chan YL, et al. Mechanisms of acute cerebral infarctions in patients with middle cerebral artery stenosis: a diffusion-weighted imaging and microemboli monitoring study. *Ann Neurol.* 2002;52(1):74-81.
35. Wu F, Zhang Q, Dong K, et al. Whole-brain magnetic resonance imaging of plaque burden and lenticulostriate arteries in patients with different types of stroke. *Ther Adv Neurol Disord.* 2019;12:175628641983329.
36. Douglas AF, Christopher S, Amankulor N, et al. Extracranial carotid plaque length and parent vessel diameter significantly affect baseline ipsilateral intracranial blood flow. *Neurosurgery.* 2011;69(4):767-773. discussion 773.
37. Zhao L, Zhao H, Xu Y, Zhang A, Zhang J, Tian C. Plaque length predicts the incidence of microembolic signals in acute anterior circulation stroke. *Dis Markers.* 2021;2021:1-7.
38. Zhao DL, Deng G, Xie B, et al. High-resolution MRI of the vessel wall in patients with symptomatic atherosclerotic stenosis of the middle cerebral artery. *J Clin Neurosci.* 2015;22(4):700-704.
39. Sitzer M, Müller W, Siebler M, et al. Plaque ulceration and lumen thrombus are the main sources of cerebral microemboli in high-grade internal carotid artery stenosis. *Stroke* 1995;26(7):1231-1233.
40. Yoshimura S, Toyoda K, Kuwashiro T, et al. Ulcerated plaques in the aortic arch contribute to symptomatic multiple brain infarction. *J Neurol Neurosurg Psychiatry.* 2010;81(12):1306-1311.
41. Kröner ES, van Velzen JE, Boogers MJ, et al. Positive remodeling on coronary computed tomography as a marker for plaque vulnerability on virtual histology intravascular ultrasound. *Am J Cardiol.* 2011;107(12):1725-1729.
42. Liang J, Guo J, Liu D, Shi C, Luo L. Application of high-resolution CUBE sequence in exploring stroke mechanisms of atherosclerotic stenosis of middle cerebral artery. *J Stroke Cerebrovasc Dis.* 2019;28(1):156-162.
43. Song JW, Pavlou A, Xiao J, Kasner SE, Fan Z, Messe SR. Vessel wall magnetic resonance imaging biomarkers of symptomatic intracranial atherosclerosis: a meta-analysis. *Stroke.* 2021;52(1):193-202.
44. Zhang DF, Chen YC, Chen H, et al. A high-resolution MRI study of relationship between remodeling patterns and ischemic stroke in patients with atherosclerotic middle cerebral artery stenosis. *Front Aging Neurosci.* 2017;9:140.
45. Shi MC, Wang SC, Zhou HW, et al. Compensatory remodeling in symptomatic middle cerebral artery atherosclerotic stenosis: a high-resolution MRI and micro-emboli monitoring study. *Neurol Res.* 2012;34(2):153-158.
46. Wong KSL, Chen C, Fu J, et al. Clopidogrel plus aspirin versus aspirin alone for reducing embolisation in patients with acute symptomatic cerebral or carotid artery stenosis (CLAIR study): a randomised, open-label, blinded-endpoint trial. *Lancet Neurol.* 2010;9(5):489-497.
47. Markus HS, Droste DW, Kaps M, et al. Dual antiplatelet therapy with clopidogrel and aspirin in symptomatic carotid stenosis evaluated using Doppler embolic signal detection: the Clopidogrel and Aspirin for Reduction of Emboli in Symptomatic Carotid Stenosis (CARESS) trial. *Circulation.* 2005;111(17):2233-2240.
48. Fisher CM, Gore I, Okabe N, White PD. Calcification of the carotid siphon. *Circulation.* 1965;32(4):538-548.
49. Muller-Kuppers M, Graf KJ, Pessin MS, DeWitt L, Caplan L. Intracranial vertebral artery disease in the new england medical center posterior circulation registry. *Eur Neurol.* 1997;37(3):146-156.
50. Wityk RJ, Chang HM, Rosengart A, et al. Proximal extracranial vertebral artery disease in the new england medical center posterior circulation registry. *Arch Neurol.* 1998;55(4):470-478.

Association of Plaque Morphology With Stroke Mechanism in Patients With Symptomatic Posterior Circulation ICAD

Xiaoyan Song, Shuang Li, Heng Du, et al.

Neurology 2022;99;e2708-e2717 Published Online before print October 11, 2022
DOI 10.1212/WNL.0000000000201299